Research Article | Vol. 29, No. 25 / 6 Dec 2021 / Optics Express 41206
Optics EXPRESS

# High resolution graphene angle sensor based on ultra-narrowband optical perfect absorption

YIMING CHEN, YANSONG FAN, ZHENGZHUO ZHANG, ZHIHONG ZHU, KEN LIU, JIANFA ZHANG, WEI XU, XIAODONG YUAN, AND CHUCAI GUO*

*College of Advanced Interdisciplinary Studies & Hunan Provincial Key Laboratory of Novel Nano-Optoelectronic Information Materials and Devices, National University of Defense Technology, Changsha, Hunan 410073, China*
*gcc_1981@163.com

**Abstract:** We propose and experimentally demonstrate high resolution angle sensors based on ultra-narrowband graphene perfect absorbers. Perfect absorption at wavelength of 1452.8 nm with absorption bandwidth of 0.8 nm is numerically demonstrated for a designed angle sensor based on single graphene absorber at normal incidence, and the angular width of the resonant absorption is only 0.05°. In the experiment, peak absorption over 95% with bandwidth about 2.8 nm is measured at normal incidence for a fabricated graphene sensor, and the device has a wavelength-angle sensitivity over 17 nm per degree which agrees well with the simulation result. Meanwhile, an optoelectronic angle sensor with high resolution and fast response by using an array of graphene absorbers is proposed. The demonstrated graphene angle sensors with ultra compact size and high resolution could be of valuable applications in many fields.



## 1. Introduction

Over the last two decades, numerous significant progresses have been made in the field of angle sensors, and many kinds of angle sensors have been developed [1]. Among various angle sensors, optical angle sensors have the advantages of high resolution and non-contact measurement, and they are also immune to electromagnetic interferences. However, the size of traditional angle sensors is relatively large, and the resolution of the angle sensors normally decrease seriously along with the decrease of the device size. Therefore, the miniaturization of angle sensors is a great challenge, and the angle sensors in a small footprint with high-performance are highly desirable.

Spectrally selective optical absorbers can be applied in miniaturized angle sensors. Metallic absorbers for angle sensing were experimentally demonstrated in the near infrared (IR), absorption bandwidth over 12 nm and wavelength-angle sensitivity near 15 nm per degree were measured [2]. Meanwhile, optical absorbers with narrow absorption band have been experimentally demonstrated [3–5]. Compared to metallic absorbers, graphene absorbers have many advantages in the application of sensing. Firstly, graphene absorbers can work in different wavelength bands since graphene has ultra-wide absorption spectrum [6]. Secondly, graphene absorbers can transfer input light into electronic signals fast [7], so graphene absorbers can be utilized as high speed optoelectronic sensors. Thirdly, the absorption bandwidth of graphene absorbers could be much narrower than that of metallic absorbers, and the narrow bandwidth is particularly important for the resolution of optical sensors.

Although graphene absorbers have many advantages, the absorption of normal graphene absorbers is very low due to the atomic thickness of graphene [8]. In order to solve this problem, graphene perfect absorbers have been proposed and studied intensively [9–22]. Recently, some applications of graphene perfect absorbers have been demonstrated [23–28], but the applications

#443842 https://doi.org/10.1364/OE.443842
Journal © 2021 Received 20 Sep 2021; revised 3 Nov 2021; accepted 17 Nov 2021; published 29 Nov 2021

Optics EXPRESS

of those absorbers are at the early stage and how to realize perfect absorption in an ultra-narrow spectral band is still very challenging.

In this work, we present a high resolution angle sensor by using a graphene perfect absorber with ultra-narrow absorption band and ultra-high wavelength-angle sensitivity. Perfect absorption at wavelength of 1452.8 nm with absorption bandwidth of 0.8 nm is calculated for a designed graphene angle sensor at normal incidence. Absorption bandwidth about 2.8 nm is measured for a fabricated graphene angle sensor, and the measured bandwidth is about one order narrower than that of typical narrowband metallic absorbers [2]. The wavelength-angle sensitivity about 17 nm per degree is measured, which is the highest value ever reported for optical angle sensors or spectrally selective absorbers in the near IR to our knowledge. In addition, we propose an optoelectronic angle sensor by utilizing an array of graphene absorbers, which has the advantages of high resolution, fast response and simple measurement. The transverse dimension of the proposed graphene angle sensors is on the order of millimeter, and the longitudinal dimension is less than 3 μm, which is much smaller than that of traditional angle sensors. The demonstrated angle sensors could be of valuable applications in precision measurement, tracking system, aerospace, MEMS system and so on.

## 2. Results and discussion

The structure of the optical angle sensor based on single graphene absorber is shown in Fig. 1(a). The sensor comprises a 1D sub-wavelength polymethy1-methacrylate (PMMA) grating, a monolayer graphene, a silica layer and a gold reflection layer. When the sensor is illuminated by a light beam in the *x*-*z* plane, the incident angle ($\alpha$) can be determined accurately by measuring the absorption spectrum or absorption rate. In order to design a high-performance optical angle sensor, high absorption, narrow bandwidth and high wavelength-angle sensitivity are required.

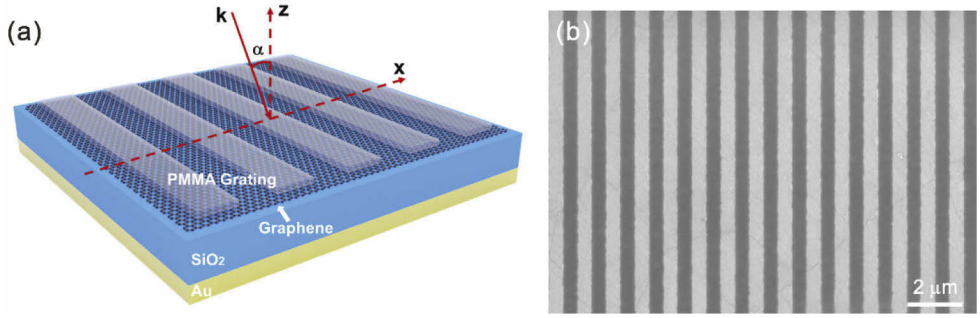


**Fig. 1.** (a) Schematic image of the optical angle sensor based on single graphene absorber. (b) SEM image of a fabricated graphene absorber.

The optical absorption of the structure shown in Fig. 1(a) can be enhanced by the guided mode resonances, and perfect absorption can be achieved at resonant wavelength under the critical coupling condition, namely the leakage rate of the resonant mode ($\gamma_l$) equal to the absorption rate of the materials ($\gamma_a$) [29–32]. Although different kinds of graphene perfect absorbers have been experimentally demonstrated [33–35], the realization of perfect absorption with an ultra-narrowband is still very challenging. In order to decrease the absorption bandwidth and maintain the high absorption, the leakage rate $\gamma_l$ and the absorption rate $\gamma_a$ should be decreased simultaneously. The thickness of PMMA grating ($t_g$) is a key parameter affecting the leakage rate $\gamma_l$ and the absorption rate $\gamma_a$ of the structure shown in Fig. 1(a). If we decrease the grating thickness close to zero, the leakage rate $\gamma_l$ of the resonant mode will decrease rapidly, but the absorption rate $\gamma_a$ will increase due to the local field enhancement, so the critical coupling condition will be broken and the peak absorption will decrease greatly. Therefore, we need

Optics EXPRESS

to decrease the absorption rate $\gamma_a$ at the same time to achieve perfect absorption with narrow bandwidth. The absorption rate $\gamma_a$ in the structure shown in Fig. 1(a) is mainly determined by the absorption of graphene, and there are some ways to control the absorption rate of graphene. For example, the absorption rate of graphene can be reduced by increasing the Fermi level of graphene with electrostatic gating [32]. However, the electrostatic gating method will make the structure more complicated. Another way to reduce the absorption rate of graphene is decreasing the optical field intensity in graphene. Increasing the thickness of the silica layer in the structure can keep graphene away from the central region of the resonant mode, so as to reduce the absorption rate of graphene.

Based on the above analysis, we designed a graphene perfect absorber with ultra-narrowband. Figure 2(a) shows the absorption spectra of a designed graphene absorber under normal incidence for transverse-electric (TE) polarization, which is calculated using finite element method-based software (COMSOL Multiphysics). As shown in the Fig. 2(a), perfect absorption at 1452.8 nm with full-width at half maximum of absorption band about 0.8 nm is achieved, and the peak absorption of the monolayer graphene and the gold layer are about 90% and 10%, respectively. In the simulation, the monolayer graphene is modeled as an anisotropic layer with a thickness of 0.34 nm, and the out-of-plane refractive index is set as $n = 1$ while the in-plane refractive index is set as $n = 3 + j5.446\lambda/3\ \mu m^{-1}$ [36]. The refractive indices of PMMA and $SiO_2$ are set as 1.48 and 1.45, the dispersion effects of PMMA and $SiO_2$ can be ignored in our calculation wavelength range [37,38]. The dielectric constant of gold is given by the Drude model as $\varepsilon(\omega) = \varepsilon_\infty - \omega_p^2/(\omega^2 + i\gamma\omega)$, $\varepsilon_\infty = 1.0$, $\omega_p = 1.37 \times 10^{16}\ s^{-1}$ and $\gamma = 8.17 \times 10^{13}\ s^{-1}$ [39]. The period of PMMA grating (P) and the grating fill factor are chosen as 1023 nm and 0.5, respectively. The thicknesses of the PMMA grating, the silica layer and the gold layer are taken to be 85 nm, 2200 nm and 200 nm, respectively. The absorption spectra of the graphene absorber for transverse-magnetic (TM) polarization are demonstrated in Supplement 1.

The perfect absorption peak shown in Fig. 2(a) is caused by a high-$Q$ resonant mode, and the normalized electric field distribution of the resonant mode excited by a normal incidence of a plane wave is shown in Fig. 2(b). The electric field of the resonant mode is well confined in the silica layer, and the electric field at the central plane of the silica layer is enhanced about 27 times. However, the electric field in the graphene layer is much lower than that of the central region of the mode, so the absorption rate $\gamma_a$ can match the low leakage rate $\gamma_l$ to satisfy the critical coupling condition.

The angular characteristics of the graphene absorber are critical when the absorber is applied as an angle sensor. Figure 2(c) shows the absorption of the absorber as a function of incident angle at wavelength of 1452.8 nm. The calculated angular width of the absorber is around 0.05°, which is much narrower than that of the metallic absorbers [2]. The incident angle can be measured with ultra-high resolution by measuring the absorption of the absorber at a fixed wavelength, but the angle measurement range is very small due to the ultra-narrow absorption band of the absorber. The incident angle can be also determined by measuring the absorption spectrum of the absorber. Figure 2(d) shows the absorption of the absorber as functions of wavelength and incident angle. As shown in Fig. 2(d), the absorption spectrum is very sensitive to the incident angle. At oblique incidence, there will be two absorption peaks, and the wavelengths of the two absorption peaks move to the long wavelength and the short wavelength respectively at almost the same speed. The wavelength-angle sensitivity ($d\lambda/d\alpha$) of the absorber is as high as 17.2 nm per degree. The wavelengths of the absorption peaks depends on the wavelengths of the resonant modes in the absorber. We use low refractive index materials (PMMA and $SiO_2$) as the grating and waveguide layer in our designed graphene abosrber, and the frequencies of the resonant modes in a periodic structure with low refractive indices change rapidly with the change of propagation constant $\beta$ ($\beta = k \cdot \sin\alpha$) [40]. So the wavelengths of the absorption peaks shift rapidly with the change of incident angle $\alpha$.

Optics EXPRESS

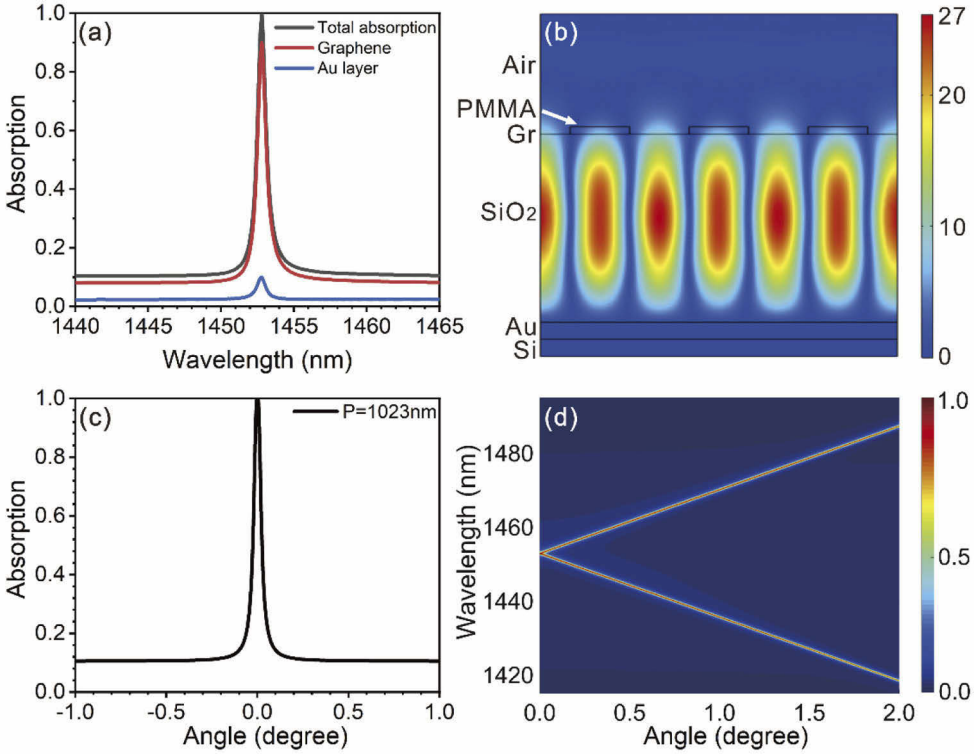


**Fig. 2.** (a) Absorption spectra of a designed graphene absorber under normal incidence for TE polarization. (b) Normalized electric field distribution of the absorber under normal incidence of a plane wave with on-resonant wavelength. (c) Absorption of the absorber as a function of incident angle at wavelength of 1452.8 nm. (d) Absorption of the absorber as functions of wavelength and incident angle.

The designed graphene angle sensor is fabricated on a silicon substrate, and a scanning electron micrograph (SEM) of the fabricated device is shown in Fig. 1(b). The lateral size of the fabricated device is 1500 μm. The absorption spectra of the fabricated graphene angle sensor at different incident angles are measured by our homebuilt microscope measurement setup (The details of the fabrication processes as well as the measurement setup and method are shown in Supplement 1). As shown in Fig. 3(a), peak absorption of 95% at wavelength of 1450.8 nm with absorption bandwidth of 2.8 nm was measured. At oblique incidence, two absorption peaks were observed, and the two peaks shift to long wavelength and short wavelength respectively as the incident angle increases. At incident angle of 2 degree, the two absorption peaks shifted to 1417.7 nm and 1485.0 nm respectively, so the measured wavelength-angle sensitivity of the angle sensor is about 17 nm per degree. Figure 3(b) shows the calculated absorption spectra of the graphene angle sensor at different incident angles, which agree well with the measured results except for the absorption bandwidth. The incident light used in the simulation is a plane wave, while the incident light in the experiment is a Gaussian beam with a small angle range. Since the absorber is very sensitive to the incident angle, the measured absorption bandwidth is wider than that of the simulation. Meanwhile, PMMA and silica are considered to be lossless in the simulation, but in the experiment, they have weak absorption and may broaden the absorption bandwidth either.

The incident angle information can be obtained in a large measurement range by measuring the absorption spectrum of the sensor based on single graphene absorber. However, the measurement

Optics EXPRESS

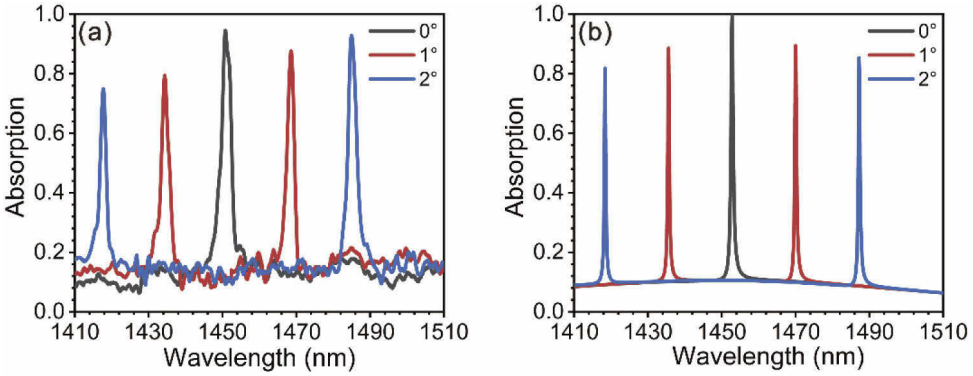


**Fig. 3.** Measured (a) and simulated (b) absorption spectra of a fabricated graphene absorber at incident angle of 0, 1, and 2 degree.

of the absorption spectrum is time-consuming. In order to realize fast angle measurement with high resolution, we propose an optoelectronic angle sensor using an array of graphene absorbers. The schematic of the optoelectronic angle sensor is shown in Fig. 4(a). The angle sensor comprises a number of graphene absorbers with different grating periods, and the graphene strip in each absorber is connected with two metal electrodes.

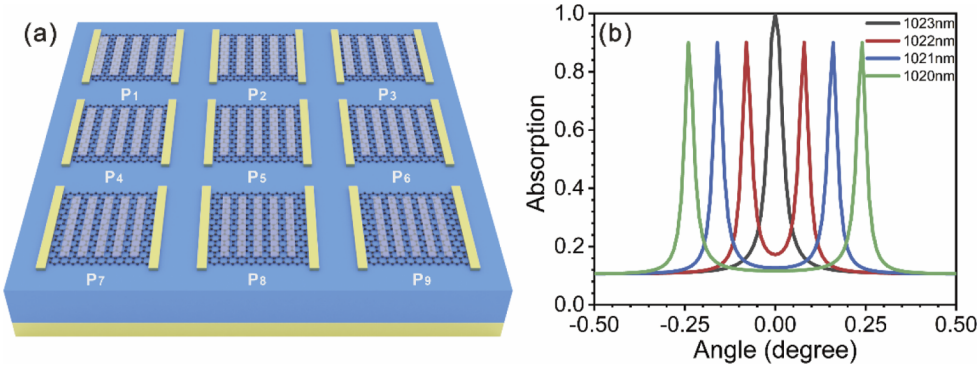


**Fig. 4.** (a) Schematic image of the optoelectronic angle sensor based on an array of graphene absorbers. (b) Simulated absorption of graphene absorbers with different periods as a function of incident angle at wavelength of 1452.8 nm.

The peak absorption wavelength of the graphene absorber is sensitive to the incident angle and the grating period, so the graphene absorbers with different grating periods can selectively absorb the incident light with a fixed wavelength at different incident angles. The periods of the graphene absorbers in the optoelectronic angle sensor should be selected according to the working wavelength. For example, if we choose the working wavelength of 1452.8 nm, the period of the first absorber can be set as 1023 nm, and the periods of the remaining absorbers decrease successively at intervals of about 1 nm. Figure 4(b) shows the absorption of four graphene absorbers with different grating periods as a function of the incident angle at incident wavelength of 1452.8 nm. As shown in Fig. 4(b), the incident angle can be precisely determined by comparing the absorptions of graphene absorbers. Meanwhile, graphene can convert absorbed input light into photocurrent in a short time, so the incident angle can be measured fast by measuring the photocurrents of the graphene absorbers.

Optics EXPRESS

## 3. Summary

In conclusion, we proposed and experimentally demonstrated an optical angle sensor with ultra-compact size and high resolution based on an ultra-narrowband graphene perfect absorber. In the simulation, perfect absorption at wavelength of 1452.8 nm with absorption bandwidth of 0.8 nm is achieved for a designed angle sensor under normal incidence, and the angular width of the resonant absorption and the wavelength-angle sensitivity are 0.05° and 17.2 nm per degree respectively. In the experiment, peak absorption over 95% with absorption bandwidth about 2.8 nm is demonstrated for a fabricated sample, and the measured wavelength-angle sensitivity agrees well with the simulated value. Meanwhile, we proposed an optoelectronic angle sensor based on an array of graphene absorbers, and the angle information can be achieved fast and precisely by measuring the photocurrent of the graphene absorbers.

**Funding.** National Natural Science Foundation of China (61404174).

**Disclosures.** The authors declare no conflicts of interest.

**Data availability.** Data underlying the results presented in this paper can be obtained from the authors upon reasonable request.

**Supplemental document.** See Supplement 1 for supporting content.

## References

1. A. S. A. Kumar, B. George, and S. C. Mukhopadhyay, "Technologies and Applications of Angle Sensors: A Review," IEEE Sens. J. **21**(6), 7195–7206 (2021).
2. Y. Qu, Q. Li, H. Gong, K. Du, S. Bai, D. Zhao, H. Ye, and M. Qiu, "Spatially and Spectrally Resolved Narrowband Optical Absorber Based on 2D Grating Nanostructures on Metallic Films," Adv. Opt. Mater. **4**(3), 480–486 (2016).
3. Z. Ren, Y. Sun, Z. Lin, and C. Wang, "Ultra-narrow band perfect metamaterial absorber based on dielectric-metal periodic configuration," Opt. Mater. **89**, 308–315 (2019).
4. S. Kang, Z. Qian, V. Rajaram, S. D. Calisgan, A. Alù, and M. Rinaldi, "Ultra-Narrowband Metamaterial Absorbers for High Spectral Resolution Infrared Spectroscopy," Adv. Opt. Mater. **7**(2), 1801236 (2019).
5. J. Yu, B. Ma, A. Ouyang, P. Ghosh, H. Luo, A. Pattanayak, S. Kaur, M. Qiu, P. Belov, and Q. Li, "Dielectric super-absorbing metasurfaces via PT symmetry breaking," Optica **8**(10), 1290–1295 (2021).
6. K. S. Novoselov, A. K. Geim, S. V. Morozov, D. Jiang, Y. Zhang, S. V. Dubonos, I. V. Grigorieva, and A. A. Firsov, "Electric Field Effect in Atomically Thin Carbon Films," Science **306**(5696), 666–669 (2004).
7. F. N. Xia, T. Mueller, Y. M. Lin, A. Valdes-Garcia, and P. Avouris, "Ultrafast graphene photodetector," Nat. Nanotechnol. **4**(12), 839–843 (2009).
8. R. R. Nair, P. Blake, A. N. Grigorenko, K. S. Novoselov, T. J. Booth, T. Stauber, N. M. R. Peres, and A. K. Geim, "Fine Structure Constant Defines Visual Transparency of Graphene," Science **320**(5881), 1308 (2008).
9. S. Thongrattanasiri, F. H. Koppens, and F. J. G. de Abajo, "Complete optical absorption in periodically patterned graphene," Phys. Rev. Lett. **108**(4), 047401 (2012).
10. Y. Liu, A. Chadha, D. Zhao, J. R. Piper, Y. Jia, Y. Shuai, L. Menon, H. Yang, Z. Ma, S. Fan, F. Xia, and W. Zhou, "Approaching total absorption at near infrared in a large area monolayer graphene by critical coupling," Appl. Phys. Lett. **105**(18), 181105 (2014).
11. M. Grande, M. A. Vincenti, T. Stomeo, G. V. Bianco, D. de Ceglia, N. Akozbek, V. Petruzzelli, G. Bruno, M. De Vittorio, M. Scalora, and A. D'Orazio, "Graphene-based perfect optical absorbers harnessing guided mode resonances," Opt. Express **23**(16), 21032–21042 (2015).
12. F. Gao, Z. Zhu, W. Xu, J. Zhang, C. Guo, K. Liu, X. Yuan, and S. Qin, "Broadband wave absorption in single-layered and nonstructured graphene based on far-field interaction effect," Opt. Express **25**(9), 9579–9586 (2017).
13. X. Jiang, T. Wang, S. Xiao, X. Yan, and L. Cheng, "Tunable ultra-high-efficiency light absorption of monolayer graphene using critical coupling with guided resonance," Opt. Express **25**(22), 27028–27036 (2017).
14. X. Feng, J. Zou, W. Xu, Z. Zhu, X. Yuan, J. Zhang, and S. Qin, "Coherent perfect absorption and asymmetric interferometric light-light control in graphene with resonant dielectric nanostructures," Opt. Express **26**(22), 29183–29191 (2018).
15. X. Zou, G. Zheng, J. Cong, L. Xu, Y. Chen, and M. Lai, "Polarization-insensitive and wide-incident-angle optical absorber with periodically patterned graphene-dielectric arrays," Opt. Lett. **43**(1), 46–49 (2018).
16. X. Cao, Y. Zhang, Z. Han, W. Li, G. Liu, Z. Xue, Y. Jin, and A. Wu, "Perfect near-infrared absorption of graphene with hybrid dielectric nanostructures," J. Mater. Sci.: Mater. Electron. **31**(8), 5820–5826 (2020).
17. Q. Li, J. Lu, P. Gupta, and M. Qiu, "Engineering Optical Absorption in Graphene and Other 2D Materials: Advances and Applications," Adv. Opt. Mater. **7**(20), 1900595 (2019).
18. X. Zhang and S. John, "Broadband light-trapping enhancement of graphene absorptivity," Phys. Rev. B **99**(3), 035417 (2019).

Optics EXPRESS


19. C. Cen, Z. Chen, D. Xu, L. Jiang, X. Chen, Z. Yi, P. Wu, G. Li, and Y. Yi, "High Quality Factor, High Sensitivity Metamaterial Graphene-Perfect Absorber Based on Critical Coupling Theory and Impedance Matching," Nanomaterials **10**(1), 95 (2020).
20. S. Lee, J. Song, and S. Kim, "Graphene perfect absorber design based on an approach of mimicking a one-port system in an asymmetric single resonator," Opt. Express **29**(19), 29631 (2021).
21. T. Liu, C. Zhou, and S. Xiao, "Tailoring anisotropic absorption in a borophene-based structure via critical coupling," Opt. Express **29**(6), 8941–8950 (2021).
22. T. Sang, S. A. Dereshgi, W. Hadibrata, I. Tanriover, and K. Aydin, "Highly Efficient Light Absorption of Monolayer Graphene by Quasi-Bound State in the Continuum," Nanomaterials **11**(2), 484 (2021).
23. Y. M. Qing, H. F. Ma, Y. Z. Ren, S. Yu, and T. J. Cui, "Near-infrared absorption-induced switching effect via guided mode resonances in a graphene-based metamaterial," Opt. Express **27**(4), 5253–5263 (2019).
24. J. Chen, S. Chen, P. Gu, Z. Yan, C. Tang, Z. Xu, B. Liu, and Z. Liu, "Electrically modulating and switching infrared absorption of monolayer graphene in metamaterials," Carbon **162**, 187–194 (2020).
25. G. C. Park and K. Park, "Tunable dual-wavelength absorption switch with graphene based on an asymmetric guided-mode resonance structure," Opt. Express **29**(5), 7307–7320 (2021).
26. A. Nematpour, N. Lisi, L. Lancellotti, R. Chierchia, and M. L. Grilli, "Experimental Mid-Infrared Absorption (84%) of Single-Layer Graphene in a Reflective Asymmetric Fabry–Perot Filter: Implications for Photodetectors," ACS Appl. Nano Mater. **4**(2), 1495–1502 (2021).
27. J. Wang, X. Mu, M. Sun, and T. Mu, "Optoelectronic properties and applications of graphene-based hybrid nanomaterials and van der Waals heterostructures," Appl. Mater. Today **16**, 1–20 (2019).
28. C. Guo, J. Zhang, W. Xu, K. Liu, X. Yuan, S. Qin, and Z. Zhu, "Graphene-Based Perfect Absorption Structures in the Visible to Terahertz Band and Their Optoelectronics Applications," Nanomaterials **8**(12), 1033 (2018).
29. J. R. Piper and S. Fan, "Total Absorption in a Graphene Monolayer in the Optical Regime by Critical Coupling with a Photonic Crystal Guided Resonance," ACS Photonics **1**(4), 347–353 (2014).
30. P. K. Sahoo, J. Y. Pae, and V. M. Murukeshan, "Enhanced absorption in a graphene embedded 1D guided-mode-resonance structure without back-reflector and interferometrically written gratings," Opt. Lett. **44**(15), 3661–3664 (2019).
31. J. Wang, A. Chen, Y. Zhang, J. Zeng, Y. Zhang, X. Liu, L. Shi, and J. Zi, "Manipulating bandwidth of light absorption at critical coupling: An example of graphene integrated with dielectric photonic structure," Phys. Rev. B **100**(7), 075407 (2019).
32. S. Xiao, T. Liu, X. Wang, X. Liu, and C. Zhou, "Tailoring the absorption bandwidth of graphene at critical coupling," Phys. Rev. B **102**(8), 085410 (2020).
33. W. Wang, A. Klots, Y. Yang, W. Li, I. I. Kravchenko, D. P. Briggs, K. I. Bolotin, and J. Valentine, "Enhanced absorption in two-dimensional materials via Fano-resonant photonic crystals," Appl. Phys. Lett. **106**(18), 181104 (2015).
34. C. C. Guo, Z. H. Zhu, X. D. Yuan, W. M. Ye, K. Liu, J. F. Zhang, W. Xu, and S. Q. Qin, "Experimental Demonstration of Total Absorption over 99% in the Near Infrared for Monolayer-Graphene-Based Subwavelength Structures," Adv. Opt. Mater. **4**(12), 1955–1960 (2016).
35. Y. S. Fan, C. C. Guo, Z. H. Zhu, W. Xu, F. Wu, X. D. Yuan, and S. Q. Qin, "Monolayer-graphene-based perfect absorption structures in the near infrared," Opt. Express **25**(12), 13079–13086 (2017).
36. M. Bruna and S. Borini, "Optical constants of graphene layers in the visible range," Appl. Phys. Lett. **94**(3), 031901 (2009).
37. G. Beadie, M. Brindza, R. A. Flynn, A. Rosenberg, and J. S. Shirk, "Refractive index measurements of poly(methyl methacrylate) (PMMA) from 0.4-1.6 μm," Appl. Opt. **54**(31), F139–F143 (2015).
38. I. H. Malitson, "Interspecimen comparison of the refractive index of fused silica," J. Opt. Soc. Am. **55**(10), 1205–1208 (1965).
39. N. Liu, H. Liu, S. Zhu, and H. Giessen, "Stereometamaterials," Nat. Photonics **3**(3), 157–162 (2009).
40. Y. Ding and R. Magnusson, "Band gaps and leaky-wave effects in resonant photonic-crystal waveguides," Opt. Express **15**(2), 680–694 (2007).